Forschungszentrum Karlsruhe
Technik und Umwelt

Wissenschaftliche Berichte
FZKA 6213

Applicability of Approximate Weight Function Procedures to Graded Materials

T. Fett, D. Munz, Y. Y. Yang
Institut für Materialforschung

Juni 1999

FORSCHUNGSZENTRUM KARLSRUHE

Technik und Umwelt

Wissenschaftliche Berichte

FZKA 6213

Applicability of approximate weight function procedures to graded materials

T. Fett, D. Munz, Y.Y. Yang

Institut für Materialforschung

Forschungszentrum Karlsruhe GmbH, Karlsruhe

1999

Als Manuskript gedruckt

Forschungszentrum Karlsruhe GmbH
Postfach 3640, 76021 Karlsruhe

Mitglied der Hermann von Helmholtz-Gemeinschaft
Deutscher Forschungszentren (HGF)

ISSN 0947-8620

Applicability of approximate weight function procedures to graded materials

Abstract:

The weight function procedure simplifies the determination of stress intensity factors. If the weight function is known for a crack in a component of homogeneous material, the stress intensity factor can be obtained by multiplying this function by the stress distribution and integrating it along the crack length. In the case of graded materials, weight functions are hardly available in the literature.

A main point of this report is to prove whether or not the approximate procedures for the derivation of weight functions (Petroski Achenbach method and direct adjustment procedure) are valid also in the case of graded materials. In the case of the direct adjustment of weight functions to reference stress intensity factor solutions it was found that no change is necessary compared with the procedure for homogeneous materials.

Anwendbarkeit der Methoden zur Bestimmung approximativer Gewichtsfunktionen für gradierte Materialien

Kurzfassung:

Eine Methode zur Bestimmung von Spannungsintensitätsfaktoren ist die Methode der Gewichtsfunktionen. Die Gewichtsfunktion ist bei homogenem Material nur von den Geometriedaten der Komponente und des Risses abhängig. Bei inhomogenen Materialien mit ortsabhängigen elastischen Eigenschaften wird die Gewichtsfunktion noch zusätzlich von deren Verteilung in der Komponente beeinflußt. Gewichtsfunktionen für derartige Materialien sind kaum bekannt.

Der Bericht befaßt sich schwerpunktsmäßig mit der Anwendbarkeit von Näherungsmethoden zur Bestimmung der Gewichtsfunktion gradierter Materialien, wie sie auch bei homogenen Materialien angewandt werden. Im Falle der Direktanpassung der Gewichtsfunktion an Referenz-Spannungsintensitätsfaktoren zeigt sich die direkte Übertragbarkeit der bei homogenem Material angewandten Vorgehensweise.

Contents

1 Introduction

In many technical applications joints of two or more materials are used. Examples are joints of ceramics and metals or coatings on substrates. In these joints the material properties such as the Young's modulus or thermal expansion coefficient change at the interface. In recent years graded interlayers with a continuous change in the properties were discussed [1-4]. Their advantages are the avoidance of stress singularities at the free edge of the interface and possibly a better interface strength.

An assessment of joints with graded interlayers and an optimisation of the joint is based on the stresses and in case of crack propagation on the stress intensity factor K. Stress intensity factors in functionally graded materials (FGM) have been calculated for some cases [5-12]. Whereas in a homogeneous material the stress intensity factor is a function of the crack size and the applied mechanical or thermal load, in graded materials the stress intensity factor is also dependent on the variation of Young's modulus in the component.

The weight function method is a powerful method to calculate K from the stress distribution in the uncracked component. If the weight function is known for a specific geometry of a component, K can be calculated by integration of the product of the weight function with stress in the uncracked component along the crack. For homogeneous materials approximate methods for the calculation of the weight function have been developed [13]. For graded materials first results are given in [14]. In this report the general application of the weight function method is shown and some examples are presented.

A main point of this report is to prove whether or not the approximate procedures for the derivation of weight functions (Petroski Achenbach method and direct adjustment procedure) are valid also in the case of graded materials.

2 Weight functions for homogeneous materials

2.1 Weight function procedure

Most of the numerical methods for stress intensity factor computation require separate calculations for each given stress distribution and each crack length. The weight function procedure developed by Bückner [15] simplifies the determination of stress intensity factors. If the weight function is known for a crack in a component, the stress intensity factor can be obtained by multiplying this function by the stress distribution and integrating it along the crack length.

If $\sigma_n(x)$ is the normal stress distribution (see Fig. 1) and $\tau(x)$ are the shear stresses in the uncracked component along the prospective crack line of an edge crack, the stress intensity factors are given by

$$K_I = \int_0^a \sigma(x) h_I(x,a)\, dx \tag{2.1}$$

$$K_{II} = \int_0^a \tau(x) h_{II}(x,a)\, dx \tag{2.2}$$

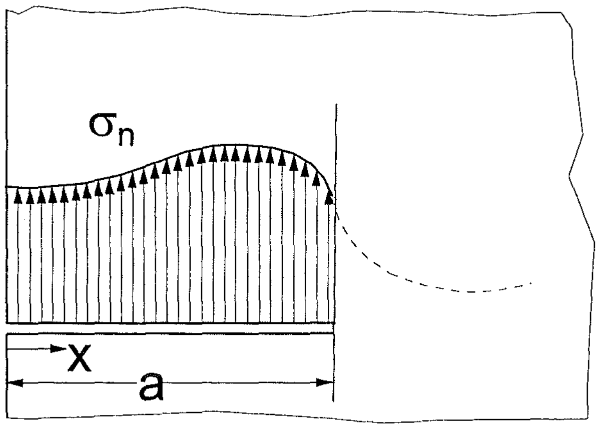

Fig. 1 Normal stresses σ_n acting on the crack faces.

The integration has to be performed over the crack length *a*. The weight function *h*(*x*,*a*) does not depend on the special stress distribution, but only on the geometry of the component.

2.2 Determination of weight functions

A possibility to compute weight functions is based on the evaluation of crack surface displacements. A relation between displacements v_r for a reference loading normal to the *x*-direction and the weight function for normal tractions, h_I, has been derived by Rice [16]

$$h_I = \frac{E}{K_{Ir}} \frac{\partial v_r}{\partial a} \tag{2.3}$$

with the mode-I reference stress intensity factor K_{Ir} and the Young's modulus E. A similar relation holds for the mode-II weight function h_{II} caused by shear tractions τ_{xy} at the crack faces

$$h_{II} = \frac{E}{K_{IIr}} \frac{\partial u_r}{\partial a} \tag{2.4}$$

with the mode-II reference stress intensity factor K_{IIr} and the crack face displacements u in x-direction. The evaluation of eqs.(2.3) and (2.4) needs the crack surface displacements for an arbitrary load and a series of crack lengths. Additionally, the related stress intensity factors for the same loading have to be known. Therefore, the determination of weight functions via eqs. (2.3) and (2.4) was often done using results of FE computations. In order to reduce the numerical effort, approximate procedures were developed, which only need reference stress intensity factors as available in fracture mechanics handbooks (see e.g. [13,17,18]). The following considerations are made for the plane stress case exclusively.

3 Approximate determination of weight functions

Two approximate procedures were developed in the past. Petroski and Achenbach [19] proposed a procedure based on an approximate description of the crack surface displacements. This method has been extended by several authors and is described in detail in handbooks on weight functions [13][20]. Another procedure, where the weight function is fitted to known reference stresses and geometrical conditions, is described in [13]. The two procedures are outlined in the following section for the case of mode-I loading

3.1 Extended Petroski Achenbach procedure

The determination of the reference crack opening displacement is based on a method first developed by Petroski and Achenbach [19]. The displacement v is calculated from the reference stress intensity factor and several geometric conditions. First, dimensionless quantities

$$\alpha = a / W, \quad \rho = x / a \tag{3.1}$$

are introduced.

The crack opening displacements can be described by

$$v(x,a) = A_0 \sum_{n=0}^{\infty} C_n (1-\rho)^{n+\frac{1}{2}} \tag{3.2}$$

with

$$A_0 = \sqrt{\frac{8}{\pi}} \frac{\sigma^*}{E} a Y_r , \quad C_0 = 1 \tag{3.3}$$

where σ^* is a characteristic value of the stress distribution and Y_r is the geometric function defined by the reference stress intensity factor K_{Ir}

$$K_{Ir} = \sigma^* Y_r \sqrt{a} \, . \tag{3.4}$$

Introducing (3.2) into (2.3) provides for the weight function [13]

$$h(x,a) = \sqrt{\frac{2}{\pi a}} \sum_{n=0}^{\infty} \left[(3-2n) C_{n-1} + (2n+1) C_n + 2 \frac{\alpha}{Y_r} \frac{dY_r}{d\alpha} C_{n-1} + 2\alpha \frac{dC_{n-1}}{d\alpha} \right] (1-\rho)^{n-\frac{1}{2}} \tag{3.5}$$

with $$C_{-1} = \frac{dC_{-1}}{d\alpha} = 0 \, .$$

3.2 Approximation of the crack opening displacement field

For practical use, the number of terms in eq.(3.2) has to be restricted. Consequently, a finite number of unknown coefficients C_n ($n > 0$) occurs. Several conditions were proposed to provide these coefficients.

3.2.1 Near-tip displacements

The first condition proposed by Petroski and Achenbach [19] considers the near-tip displacements v_N which are given by

$$v_N = \sqrt{\frac{8}{\pi}} \frac{K_{Ir}}{E} \sqrt{a-x} = A_0 \sqrt{1-\rho} \, . \tag{3.6}$$

This leads to the coefficient A_0 given in (3.3).

3.2.2 Condition of self-consistency

Another condition is an energy relation which is obtained by introducing eq.(2.3) into (2.1)

$$K_{Ir} = \frac{E}{K_{Ir}} \int_0^a \sigma_r(x) \frac{\partial v_r}{\partial a} dx \tag{3.7}$$

resulting in

$$E\int \sigma_r v_r(x,a)\,dx = \int_0^a K_{Ir}^2\,da \tag{3.8}$$

3.2.3 Second derivative of displacements

The second derivative of the displacements v must disappear at the crack mouth (x=0). This has been shown in [21] [22] by the following considerations. Let us start with the well-known relations

$$\frac{\tau_{xy}}{G} = \frac{\partial u}{\partial y} + \frac{\partial v}{\partial x} \tag{3.9}$$

$$\frac{\partial u}{\partial x} = \varepsilon_x = \frac{1}{E}(\sigma_x - \nu\sigma_y) \tag{3.10}$$

$$\frac{\partial v}{\partial y} = \varepsilon_y = \frac{1}{E}(\sigma_y - \nu\sigma_x) \tag{3.11}$$

$$\frac{\partial \sigma_y}{\partial y} = -\frac{\partial \tau_{xy}}{\partial x} \tag{3.12}$$

$$\frac{\partial \sigma_x}{\partial x} = -\frac{\partial \tau_{xy}}{\partial y} \tag{3.13}$$

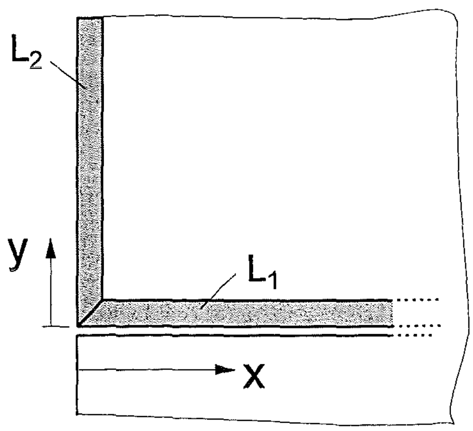

Fig. 2 Boundary conditions at the free surfaces near the crack mouth.

Taking the derivative of (3.9) with respect to x gives

$$\frac{\partial^2 v}{\partial x^2} = \frac{1}{G}\frac{\partial \tau_{xy}}{\partial x} - \frac{\partial^2 u}{\partial x \partial y} \tag{3.14}$$

and thereby

$$\frac{\partial^2 v}{\partial x^2} = \left(\frac{1}{G} - \frac{\nu}{E}\right)\frac{\partial \tau_{xy}}{\partial x} - \frac{1}{E}\frac{\partial \sigma_x}{\partial y} \tag{3.15}$$

Along the free surface L_1 it holds

$$\tau_{xy}\big|_{y=0} = \sigma_y\big|_{y=0} = 0 \quad \forall x < a \tag{3.16}$$

and along L_2

$$\tau_{xy}\big|_{x=0} = \sigma_x\big|_{x=0} = 0 \quad \forall y \tag{3.17}$$

Consequently, we obtain

$$\frac{\partial \tau_{xy}}{\partial x} = 0 \ \ \forall x < a, y = 0 \ \ \text{and} \ \ \frac{\partial \sigma_x}{\partial y} = 0 \ \ \forall y, x = 0 \tag{3.18}$$

Introducing (3.18) into (3.15) leads to

$$\left.\frac{\partial^2 v}{\partial x^2}\right|_{x=y=0} = 0 \tag{3.19}$$

3.3 Direct adjustment of weight functions to reference stress intensity factors

From the general type of the weight function, eq.(3.5), a set-up can be concluded as [23]

$$h(x,a) = \sqrt{\frac{2}{\pi a}}\left[\frac{1}{\sqrt{1-\rho}} + \sum_{n=1}^{\infty} D_n (1-\rho)^{n-\frac{1}{2}}\right] \tag{3.20}$$

For practical applications this expansion is truncated after a certain number N. From a number of N conditions, the unknown coefficients D_n can be concluded.

Let the stress intensity factor for the reference load σ_r be known. Introducing (3.20) into eq.(2.1) yields

$$K_r = \int_0^a h(x,a)\sigma_r(x)\,dx = \sigma_0\sqrt{\frac{2a}{\pi}}\left[\int_0^1 \frac{\sigma_r/\sigma_0}{\sqrt{1-\rho}}d\rho + \sum_{n=1}^{N} D_n \int_0^1 (1-\rho)^{n-1/2}(\sigma_r/\sigma_0)d\rho\right] \quad (3.21)$$

As a further condition the disappearing second (and third) derivatives of the weight function at $x=0$ can be used. It follows easily from the condition $v''=0$ at $x=0$ and $y=0$ that

$$\frac{\partial^2}{\partial x^2}h_I = \frac{E}{K_{Ir}}\frac{\partial}{\partial a}\frac{\partial^2 v}{\partial x^2} = 0\,. \quad (3.22)$$

4 Application to graded materials

As could be seen from eqs.(2.3), (3.3) and (3.8), the only material property which influences the weight function procedure is the Young's modulus E. In the special case of homogeneous materials, the weight function is trivially independent of E, since the displacements are proportional to $1/E$ and, consequently, E = const is canceled. In case of gradient materials the Young's modulus is a function of the location x. In order to apply the same treatment for non-homogeneous materials, we first have to assess the validity of the basic relations.

4.1 Basic considerations

4.1.1 Near-tip displacements

Even under varying Young's modulus $E=E(x)$, the near-tip field must be identical with that of a homogeneous material having the Young's modulus $E=E|_{x=a}=E(a)$, see e.g. [24, 25]. This fact is illustrated in Fig. 3.

Let us study the near-tip behaviour. Therefore, we take into consideration a small section of the body (dashed circle) very close to the crack tip. Then this near-tip zone is zoomed very strongly. Consequently, the outer borders of the component move to infinity. Now, we have the case of an infinite crack in an infinite body. The Young's modulus which before exhibited a finite change over the crack is now constant over the near-tip region and has the value of $E=E|_{x=a}=E(a)$. The near-tip crack opening displacement v_N for graded materials can be written as

$$v_N = \sqrt{\frac{8a}{\pi}}\frac{K_{Ir}}{E(a)}\sqrt{1-\rho} = A_0\sqrt{1-\rho} \tag{4.1}$$

where now the Young's modulus at the crack tip is entered in (3.6).

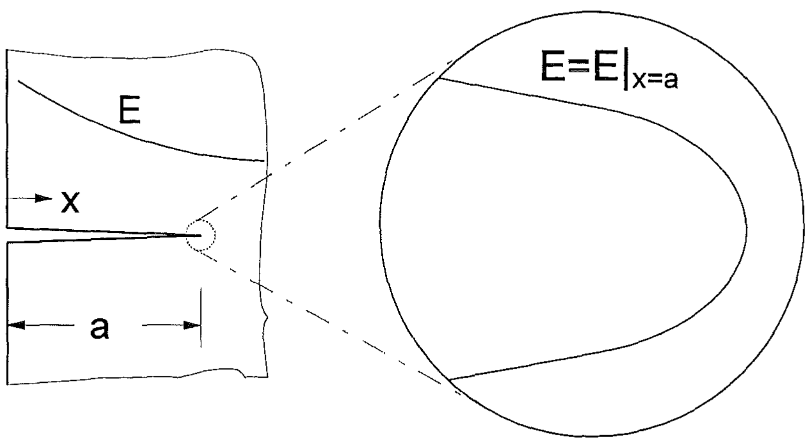

Fig. 3 Near-tip displacements under conditions of a varying Young's modulus.

4.1.2 Set-up for the crack opening displacement field

The series representation of crack opening displacement for homogeneous materials could be derived in [13] based on the Williams stress function [26]. This treatment is no longer possible for graded materials. Similar to [21], we derive an approximate set-up. The ratio between the total and the near-tip crack opening displacements

$$\frac{v}{v_N} = f(1-\rho)\,, \quad \rho = x/a \tag{4.2}$$

is a function of the argument (1-ρ) exclusively. This function can be expanded in a Taylor series at $\rho=1$

$$\frac{v}{v_N} = \sum_{n=0}^{\infty} \frac{1}{n!} f^{(n)}\Big|_{\rho=1} (1-\rho)^n\,, \quad f^{(0)}\Big|_{\rho=1} = 1 \tag{4.3}$$

Then, the total crack opening displacement is

$$v = v_N \sum_{n=0}^{\infty} C_n (1-\rho)^n\,, \quad C_n = \frac{1}{n!} f^{(n)}\Big|_{\rho=1} \tag{4.4}$$

$$v = A_0 \sum_{n=0}^{\infty} C_n (1-\rho)^{n+1/2}\,, \quad C_0 = 1 \tag{4.5}$$

where A_0 is given by eq.(3.3) with $E=E|_{x=a}$.

4.1.3 Validity of the Rice equation for graded materials

The basic relation (2.3) given by Rice [16] contains the Young's modulus. Under conditions of varying E, the question arises, which value has to be used. For this problem let us follow the considerations made in [13].

The relation between the mode-I stress intensity factor K_I and the energy release rate G_I

$$G_I = \frac{K_I^2}{E} \tag{4.6}$$

was derived by Irwin [27] on the basis of virtual crack closure in the near-tip region. Following the argumentation of [27] (see also [17]), it is self-evident that the modulus at the crack tip has to be entered in (4.6), i.e. $E=E|_{x=a}=E(a)$.

The energy release rate G_{I1} for a crack of length a under a load $\sigma_1(x)$ causing crack opening $v_1(x)$ is

$$G_{I1} = \frac{K_{I1}^2}{E(a)} = \frac{\partial}{\partial a}\int_0^a \sigma_1(x) v_1(x)\, dx \tag{4.7}$$

In a second state of loading (indicated by the subscript 2), an equivalent relation holds

$$G_{I2} = \frac{K_{I2}^2}{E(a)} = \frac{\partial}{\partial a}\int_0^a \sigma_2(x) v_2(x)\, dx \tag{4.8}$$

If the two loading cases are superimposed $\sigma_3(x) = \sigma_1(x)+\sigma_2(x)$, $v_3(x) = v_1(x)+v_2(x)$ and $K_{I3} = K_{I1} + K_{I2}$ are obtained. This gives

$$\frac{(K_{I1}+K_{I2})^2}{E(a)} = \frac{\partial}{\partial a}\int_0^a (\sigma_1+\sigma_2)(v_1+v_2)\, dx =$$

$$= \frac{\partial}{\partial a}\left[\int_0^a \sigma_1 v_1 dx + \int_0^a \sigma_2 v_2 dx + \int_0^a \sigma_2 v_1 dx + \int_0^a \sigma_1 v_2 dx\right] \tag{4.9}$$

Introducing Betti's theorem

$$\int_0^a \sigma_1 v_2\, dx = \int_0^a \sigma_2 v_1\, dx \tag{4.10}$$

gives

$$\frac{K_{I1}^2}{E(a)} + \frac{K_{I2}^2}{E(a)} + 2\frac{K_{I1}K_{I2}}{E(a)} = \frac{\partial}{\partial a}\int_0^a \sigma_1 v_1\, dx + \frac{\partial}{\partial a}\int_0^a \sigma_2 v_2\, dx + 2\frac{\partial}{\partial a}\int_0^a \sigma_2 v_1\, dx \tag{4.11}$$

Having in mind the differentiation rule

$$\frac{\partial}{\partial a}\int_0^a \sigma\, v\, dx = \int_0^a \frac{\partial(\sigma\, v)}{\partial a} dx + \sigma(a) v(a) \tag{4.12}$$

and the fact that $v(a)=0$, it is obtained from (4.11) that

$$K_{I2} = \frac{E(a)}{K_{I1}}\int_0^a \sigma_2 \frac{\partial v_1}{\partial a} dx \tag{4.13}$$

and, if we interprete the state '1' as the reference stress state 'r' and state '2' as the state for which the stress intensity factor should be computed, it is found that

$$K_I = \frac{E(a)}{K_{Ir}}\int_0^a \sigma(x) \frac{\partial v_r}{\partial a} dx = \int_0^a \sigma(x) h_I(x,a)\, dx \tag{4.14}$$

defining the weight function h_I as

$$h_I = \frac{E(a)}{K_{Ir}} \frac{\partial v_r}{\partial a} . \tag{4.15}$$

From this analysis we can conclude that in case of a graded material the Young's modulus at the crack tip has to be introduced into (2.3) and (2.4).

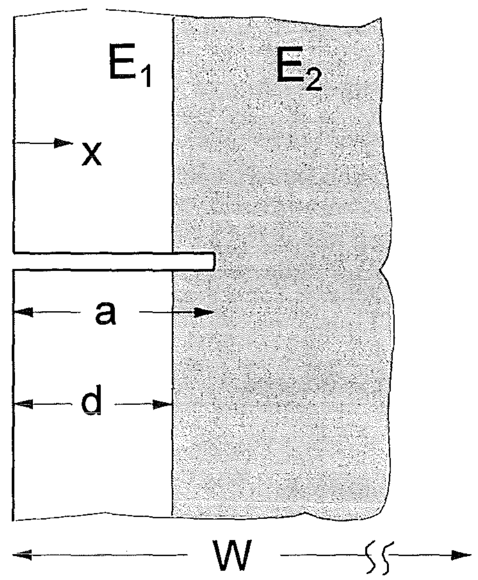

Fig. 4 Crack in a joint of dissimilar materials.

A numerical check of (4.15) has been presented in [28] for a Young's modulus given by

$$E = \begin{cases} E_1 & \text{for} \quad x < d \\ E_2 & \text{for} \quad x > d \end{cases} \tag{4.16}$$

with $E_1/E_2 = 50$, 10, and 1. The other parameters (see Fig. 4) were $d/W = 0.05$ and $a/d = 1.1$. The weight function was computed according to (4.15) from the crack opening displacement obtained by a FE analysis. In a second computation, pairs of concentrated forces P were applied to the crack faces at different locations, thus providing also the weight function as the stress intensity factor K_{IP} of these point loads. The results are intercompared in Table 1 for the special case of the weight function for $x = 0$ (i.e. the crack mouth).

These numerical results show an excellent agreement between the two independent methods for the determination of weight functions. Maximum deviations of < 0.3% are within the accuracy of the FE method.

E_2/E_1	h (4.15)	from K_P	Difference
1/1	1.45518	1.45102	-0.29%
1/10	1.22778	1.22595	0.15%
1/50	1.2627	1.2663	0.28%

Table 1 Comparison of weight functions at the crack mouth ($x = 0$) based on the J-integral and on crack opening displacements.

4.1.4 Condition of self-consistency

From eq.(4.14) the energy condition can be derived according to eq.(3.8). It now reads

$$\int_0^a \sigma_r v_r(x,a)\,dx = \int_0^a \frac{1}{E(a')} K_{Ir}^2\, da' \tag{4.17}$$

i.e. the Young's modulus occurs in the integral.

4.1.5 Second derivative of displacements

From (3.9) it now results by differentiation with respect to x

$$\frac{\partial^2 u}{\partial x \partial y} + \frac{\partial^2 v}{\partial x^2} = \frac{1}{G}\frac{\partial \tau_{xy}}{\partial x} - \frac{1}{G^2}\frac{\partial G}{\partial x}\tau_{xy} \tag{4.18}$$

and similar to (3.15) we find

$$\frac{\partial^2 v}{\partial x^2} = \left(\frac{1}{G} - \frac{\nu}{E}\right)\frac{\partial \tau_{xy}}{\partial x} - \frac{1}{G^2}\frac{\partial G}{\partial x}\tau_{xy} - \frac{1}{E}\frac{\partial \sigma_x}{\partial y}$$

Using the stress conditions (3.16)-(3.18), it follows again at the corner (x=y=0)

$$\left.\frac{\partial^2 v}{\partial x^2}\right|_{x=y=0} = 0 \tag{4.19}$$

as found for the homogeneous material.

4.2 Direct adjustment of weight functions to reference stress intensity factors

Concerning the direct adjustment method, we also look for an appropriate set-up of the weight function $h(x,a)$. Introducing the near-tip displacements v_N (4.1) into (4.15) shows that the first term of the weight function h_N, which dominates the near-tip behaviour, has the form of

$$h_N(x,a) = \sqrt{\frac{2}{\pi a}}\frac{1}{\sqrt{1-\rho}} \tag{4.20}$$

In this case, we also consider the ratio of the total weight function h and the near-tip solution h_N which is only a function of (1-ρ)

$$\frac{h}{h_N} = g(1-\rho) \tag{4.21}$$

The Taylor expansion at ρ = 1 reads

$$\frac{h}{h_N} = \sum_{n=0}^{\infty} D_n(1-\rho)^n \, , \quad D_n = \frac{1}{n!}g^{(n)}\bigg|_{\rho=1} \, , \quad D_0 = 1 \tag{4.22}$$

and, consequently,

$$h = \sqrt{\frac{2}{\pi a}}\sum_{n=0}^{\infty} D_n(1-\rho)^{n-\frac{1}{2}} \tag{4.23}$$

which is the same form as for materials with varying E. It should be mentioned that the coefficients D_n differ from those in eq.(3.20).

As a direct consequence of eqs.(4.15), (4.19) and (4.23), we obtain a disappearing second derivative of the weight function for $x = 0$

$$h''\big|_{x=0} = \frac{d^2h}{dx^2}\bigg|_{x=0} = 0 \tag{4.24}$$

5 Estimative application of weight function for homogeneous material

For the computation of stress intensity factors for thermal problems using weight function techniques, the change in material data influences both the thermal stresses σ^{th} and the weight function. For rough estimations of thermal stress intensity factors K^{th}, it is possible to evaluate the integral of eq.(2.1) by using the weight function h^{hom} for the homogeneous material, which is available from the literature (see e.g. [13])

$$K^{th} \cong \int_0^a \sigma^{th} h^{hom} dx \tag{5.1}$$

This approximation was applied to a thermal stress problem discussed by Bleek et al.[12]. Figure 5a shows the component consisting of three regions. In the layer with thickness h_1 a constant Young's modulus appears. In the ligament ($x > h_1 + h_2$) the material exhibits a constant modulus $E_2 = E_1/2$. In the interlayer of thickness h_2 the Young's modulus changes from E_1 to E_2 (see Fig. 5b) according to

$$E(x) = E_2 - (E_2 - E_1)\left(\frac{h_2 + h_1 - x}{h_2}\right)^2 \tag{5.2}$$

The thermal stresses from FE computations [12] are represented in Fig. 6a, normalised by the characteristic stress

$$\sigma^* = \alpha_1 E_1 \Delta T \tag{5.3}$$

where α_1 and E_1 are the thermal expansion coefficient and the Young' modulus of material 1 and ΔT is the change of temperature.

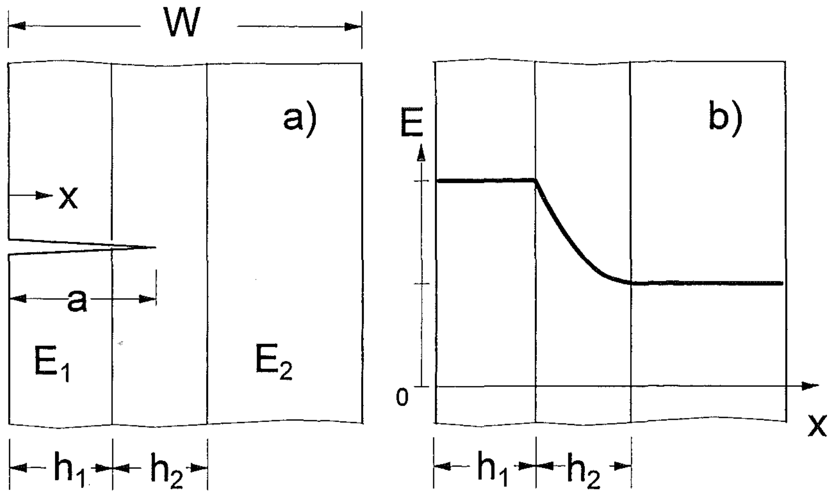

Fig. 5 a) A cracked joint with interlayer (investigated by Bleek et al. [12]), b) Change of Young's modulus across the component.

The thermal stress intensity factors K^{th} estimated from (5.1) are plotted in Fig. 5b as the curve. The squares represent the FE.results from [12]. The estimated weight function results show the same trend with relative crack size a/W as the FE results do. Nevertheless, the significant differences near $a = h_1$ of about 20% call for an improved weight function.

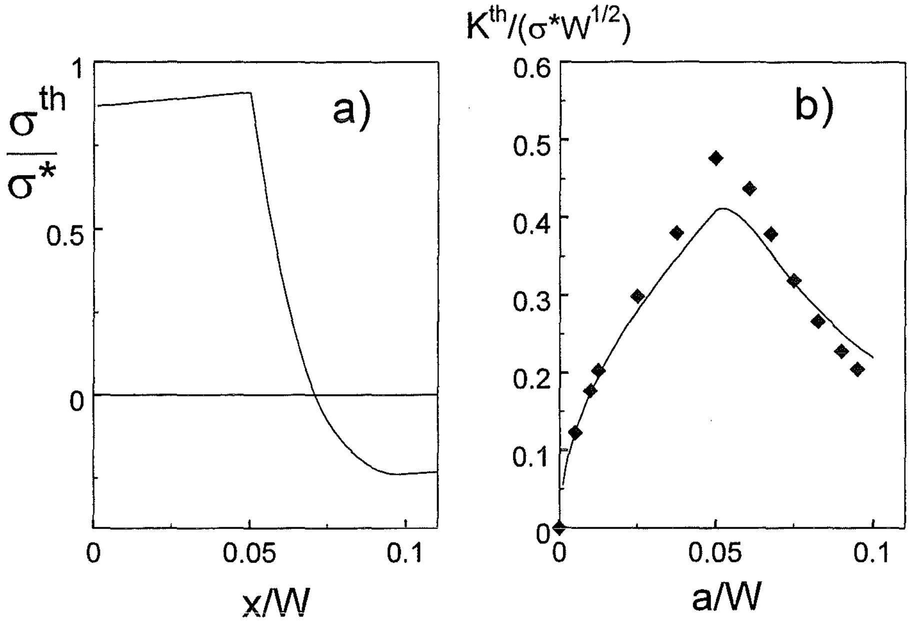

Fig. 6 a) Stresses in the uncracked joint (Fig. 5a) with a graded interlayer for h_1/W=0.05; b) stress intensity factors from FE computations [12] (symbols) and weight function computations using the weight function solution for homogeneous material (5.1).

6 Application of the direct adjustment procedure

The simplest possibility for the determination of weight functions for FGM materials is the direct adjustment method. The procedure will be explained here in detail for an edge-cracked rectangular plate.

6.1 Reference stress intensity factors

In order to explain the procedure of weight function determination, let us consider an edge-cracked plate with height-to-width ratio of $L/W = 3$ (for the geometric data see Fig. 7). In a first example, a linear change in Young's modulus E is considered with E decreasing from $E = E_0$ at $x = 0$ to $E = \frac{1}{2}E_0$ at $x = W$ by

$$E(x) = E_0(1 - \tfrac{1}{2}x / W) \tag{6.1}$$

Two reference loading cases are chosen as illustrated by Figs. 7a and 7b. In the first reference loading case the crack faces are loaded by the constant pressure σ (see Fig. 7a). The second loading case is a pair of concentrated forces P acting at the crack mouth $x = 0$ (see Fig. 7b).

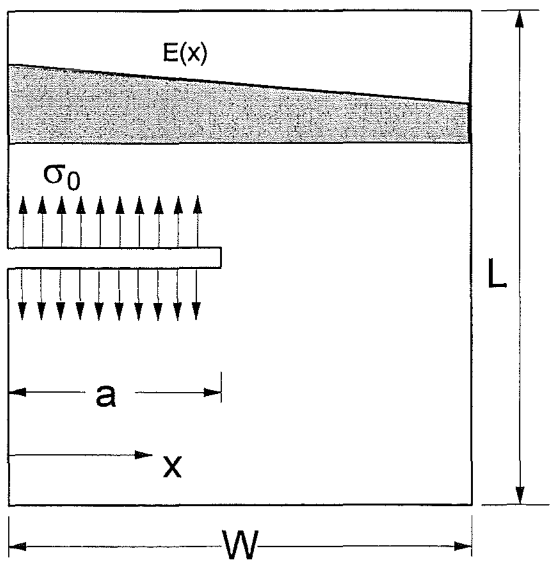

Fig. 7a First reference loading case: constant crack-face pressure.

The reference stress intensity factors obtained by FE computations are compiled in Table 2 for several relative crack depths a/W. These data may be the basis for further considerations.

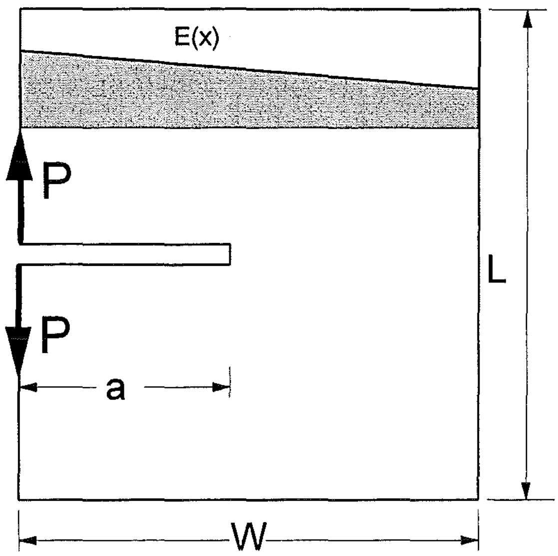

Fig. 7b Second reference loading case: concentrated forces at the crack mouth.

a/W	$K_\sigma / (\sigma\sqrt{W})$	$K_P\sqrt{W} / P$
0.2	1.1324	5.1902
0.4	2.5419	7.5950
0.5	3.8163	10.2009
0.6	5.9538	14.648
0.7	10.0474	23.1287
0.8	19.8947	43.3881

Table 2 Reference stress intensity factors for constant crack-face loading (K_σ) and for a pair of concentrated forces P at the crack mouth (K_P). Change in Young's modulus according to eq.(6.1).

6.2 Computation of the weight function

6.2.1 Three-terms approximation

A weight function with three terms reads

$$h = \sqrt{\frac{2}{\pi a}}\left[\frac{1}{\sqrt{1-\rho}} + D_1\sqrt{1-\rho} + D_2(1-\rho)^{3/2}\right] \tag{6.2}$$

From the first loading case we obtain the condition of

$$\int_0^a h(x,a)\sigma(x)\,dx = K_\sigma \tag{6.3}$$

The second loading case provides

$$h(x=0,a) = K_P / P \tag{6.4}$$

Introducing eq.(6.2) into (6.3) and (6.4) yields a system of two linear equations

$$\frac{2}{3}D_1 + \frac{2}{5}D_2 = \sqrt{\frac{\pi}{2a}}\frac{K_\sigma}{\sigma} - 2 \tag{6.5a}$$

$$D_1 + D_2 = \sqrt{\frac{\pi a}{2}}\frac{K_P}{P} - 1 \tag{6.5b}$$

from which the two coefficients D_1 and D_2 can be computed. The system (6.5) provides the coefficients compiled in Table 3.

a/W	D_1	D_2
0.2	1.53716	0.37194
0.4	3.85875	1.16154
0.5	5.80478	2.23553
0.6	8.7941	4.42637
0.7	14.0626	9.1906
0.8	25.5829	22.055

Table 3 Coefficients of a 3-terms weight function according to eq.(6.2) and Table 2.

6.2.2 Four-terms weight function

If we use the additional crack mouth condition with a disappearing second derivative ($h''_{x=0}=0$, see eq.(4.24)), a 4-terms weight function can be obtained. This weight function reads

$$h = \sqrt{\frac{2}{\pi a}}\left[\frac{1}{\sqrt{1-\rho}} + D_1\sqrt{1-\rho} + D_2(1-\rho)^{3/2} + D_3(1-\rho)^{5/2}\right] \tag{6.6}$$

with the coefficients resulting from the system of linear equations as

$$\frac{2}{3}D_1 + \frac{2}{5}D_2 + \frac{2}{7}D_3 = \sqrt{\frac{\pi}{2a}}\frac{K_\sigma}{\sigma} - 2 \tag{6.7a}$$

$$D_1 + D_2 + D_3 = \sqrt{\frac{\pi a}{2}} \frac{K_P}{P} - 1 \tag{6.7b}$$

$$D_1 - 3D_2 - 15D_3 = 3 \tag{6.7c}$$

where the third relation reflects the disappearing second derivative. The coefficients obtained from (6.7) are compiled in Table 4.

a/W	D_1	D_2	D_3
0.2	1.42972	0.73008	-0.250702
0.4	3.74934	1.52625	-0.255293
0.5	5.64221	2.77745	-0.379342
0.6	8.48223	5.46595	-0.727708
0.7	13.3742	11.4836	-1.60511
0.8	23.767	28.1081	-4.23715

Table 4 Coefficients of a 4-terms weight function according to eq.(6.6) and Table 2.

6.2.3 Check of the approximate weight functions by FE computations

In order to prove the accuracy of the approximate weight functions, additional FE computations were performed. The weight function in the range of $0 < x < a$ was computed as the stress intensity factor for a pair of concentrated forces at location $x = d$ (see Fig. 8). This is possible since the weight function is the Green's function for stress intensity factors.

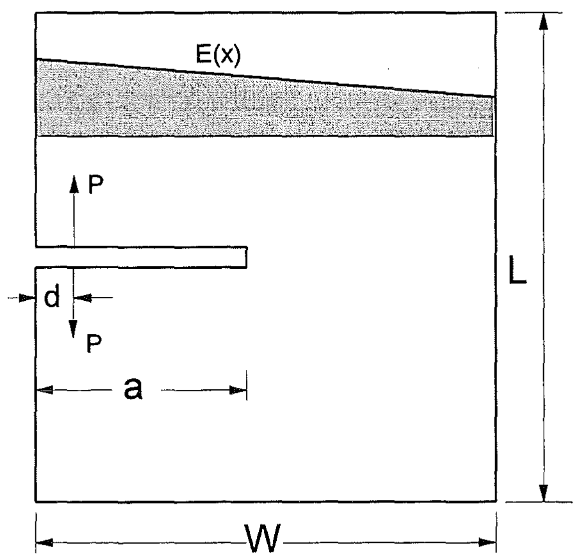

Fig. 8 Check of the weight function by stress intensity factors for concentrated forces.

The identity of the weight function and the Green's function can be shown easily by expressing the concentrated forces P (which for a constant plate thickness B are in principle line loads P/B) by the stress distribution of

$$\sigma(x) = \frac{P}{B}\delta(x-d) \tag{6.8}$$

with the Dirac delta function δ. Introducing this stress into eq.(2.1) gives

$$K_P = \frac{P}{B}\int_0^a h(x,a)\delta(x-d)\,dx = \frac{P}{B}h(d,a) \tag{6.9}$$

and replacing B by the unit thickness

$$h(d,a) = K_P / P. \tag{6.10}$$

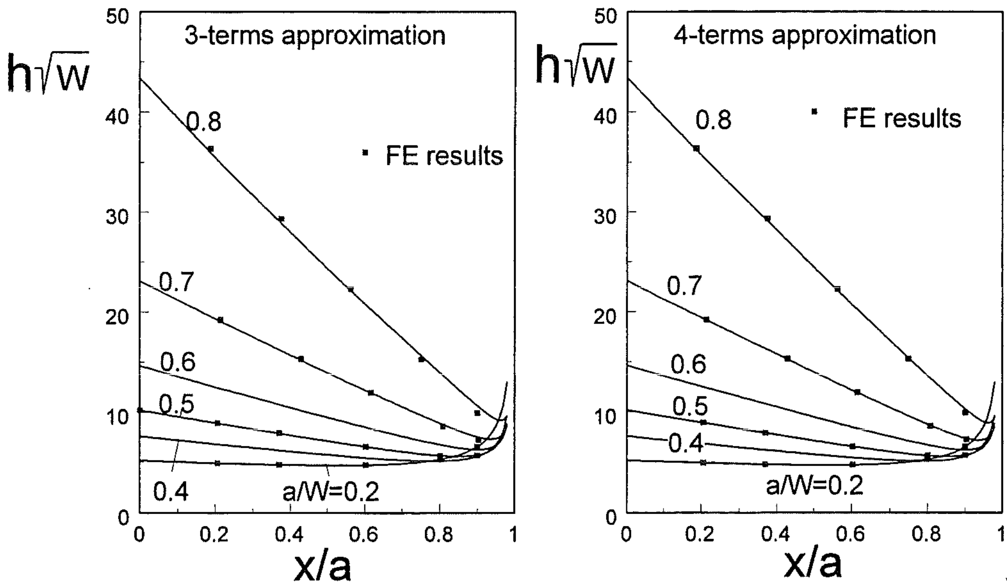

Fig. 9 Comparison of approximate weight functions (curves) with FE results (squares). Change in Young's modulus according to eq.(6.1).

Figure 9 shows the approximate weight functions according to eqs.(6.2) and (6.6) as curves together with the FE results represented by the symbols. An excellent agreement is obvious for both approximate weight functions for $a/W < 0.7$. The 4-terms approximation exhibits best agreement with the FE results also at the large crack depth of $a/W = 0.8$.

In another case, the differences in Young's moduli were increased drastically according to

$$E(x) = E_0(1 - \tfrac{49}{50}x/W) \tag{6.11}$$

The reference loading cases now yielded the data of Table 5 and by the use of eqs.(6.5) and (6.7) the coefficients listed in Tables 6 and 7. Using these data the weight functions were computed and are shown in Fig. 10. Also in this case, the derived weight function is in best agreement with the FE results.

a/W	$K_\sigma / (\sigma\sqrt{W})$	$K_P\sqrt{W} / P$
0.2	1.2629	6.2407
0.4	3.1717	10.2934
0.5	5.0025	14.3891
0.6	8.1611	21.3091
0.7	14.3087	34.427
0.8	29.0633	65.1378

Table 5 Reference stress intensity factors for constant crack-face loading (K_σ) and for a pair of concentrated forces P at the crack mouth (K_P). Change of Young's modulus according to eq.(6.11).

a/W	D_1	D_2
0.2	2.02541	0.4725
0.4	5.33083	1.8284
0.5	8.12211	3.6299
0.6	12.4874	7.1997
0.7	20.6687	14.4314
0.8	37.1893	34.8301

Table 6 Coefficients of a 3-terms weight function according to eq.(6.2) and Table 5.

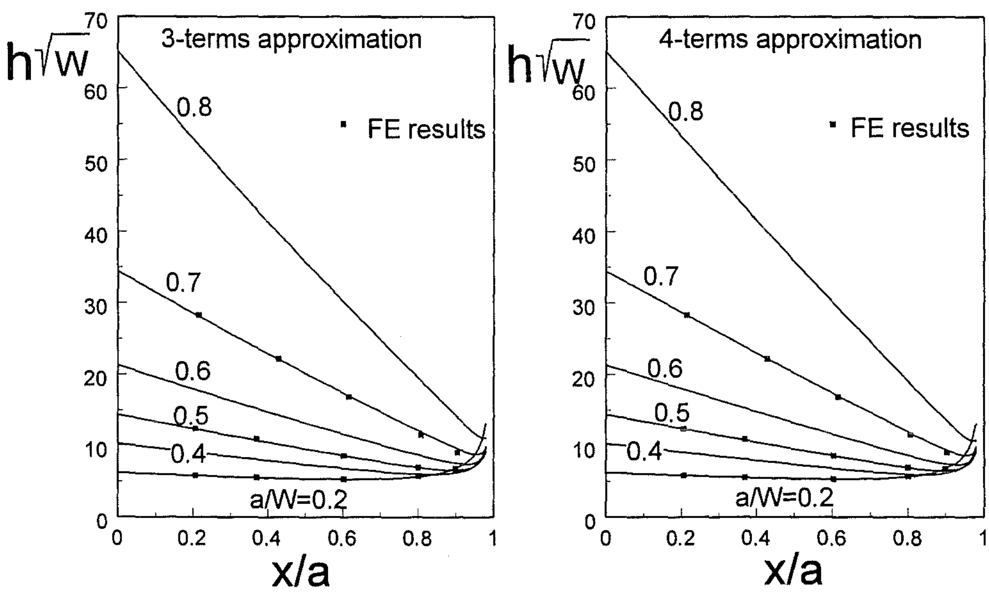

Fig. 10 Comparison of approximate weight functions (curves) with FE results (squares). Change in Young's modulus according to eq.(6.11).

a/W	D_1	D_2	D_3
0.2	1.92574	0.80473	-0.232564
0.4	5.19939	2.2665	-0.30667
0.5	7.8818	4.43094	-0.56074
0.6	11.9828	8.88194	-1.17754
0.7	19.601	17.9905	-2.49137
0.8	34.260	44.5941	-6.83482

Table 7 Coefficients of a 4-terms weight function according to eq.(6.6) and Table 5.

6.3 Comparison with the weight function for homogeneous plates

In Section 5 the unknown weight function for a FGM plate was tentatively replaced by the weight function for a homogeneous plate. In this case, the agreement between the results obtained with this weight function and the FE results was astonishingly good.

Next, the inverse linear transition function was considered where the Young's modulus increases from the value E_0 at x=0 to the value $2E_0$ at x=W, i.e.

$$E(x) = E_0(1 + x / W) \tag{6.12}$$

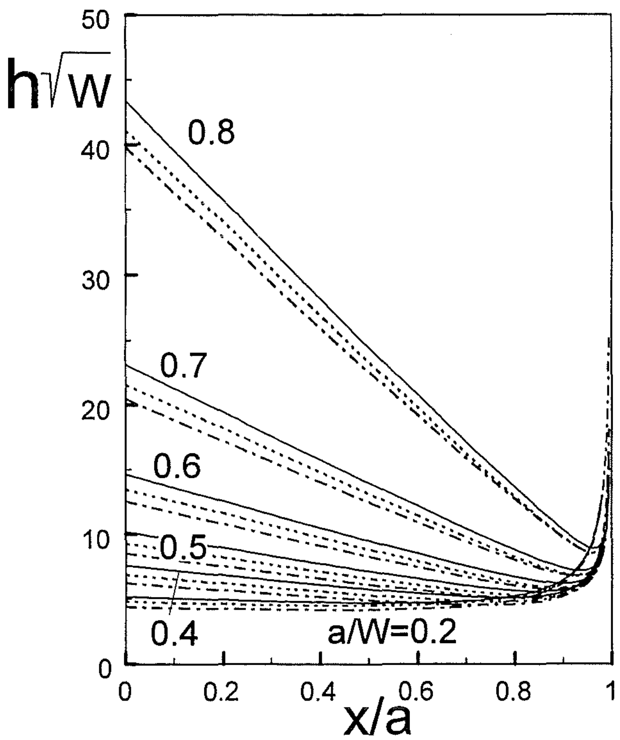

Fig. 11 Comparison between weight function for FGM and the weight function for homogeneous material [13] (dashed lines). Solid curves: transition function eq.(6.1); dash-dotted curves: transition function eq.(6.12).

In this section, the weight function for the FGM problem is now compared with the weight function available for homogeneous material [13]. Figure 11 represents the FGM weight function (solid curves for eq.(6.1), dash-dotted curves for eq.(6.12)) and the weight function from [13] (dashed curves).

The weight function for the FGM plate with linearly decreasing Young's modulus slightly exceeds that of homogeneous material. The weight function for a linearly increasing Young's modulus is slightly below the weight function for the constant E. Having this in mind, the results of Section 5 can be understood.

6.4 Non-linear change of Young's modulus

In the case of linear E-distributions over the plate width W, an excellent agreement between the weight functions obtained by direct adjustment to reference loading cases and from FE computations was found. In order to prove the weight function for a more complicated material behaviour, we tested the procedure for other dependencies of $E(x)$ as well:

$$E = E_0[1 - \tfrac{49}{50}(x/W)^{0.3}] \tag{6.13}$$

$$E = E_0[1 - \tfrac{49}{50}(x/W)^{3}] \tag{6.14}$$

Figure 12 illustrates these relations. In all cases the Poisson ratios were not graded and kept constant ($\nu = 0.3$).

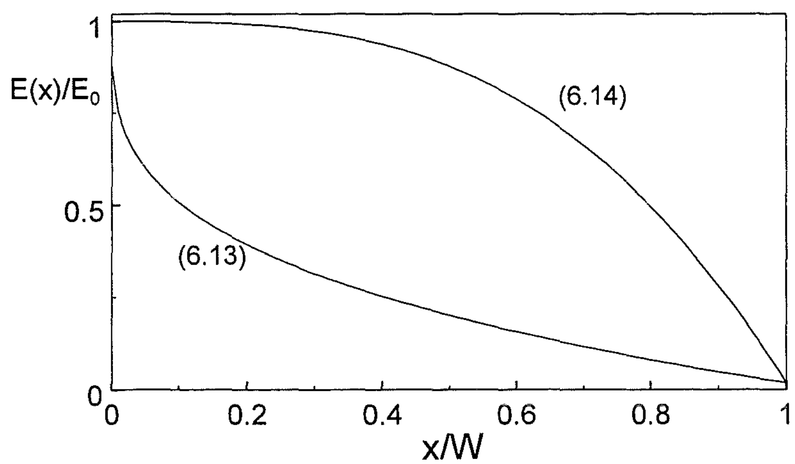

Fig. 12 Transition functions for the Young's modulus according to eqs.(6.13) and (6.14).

The obtained weight functions with 4 terms are plotted in Fig 13. By comparing the curves with FE results (squares), best agreement is found in these cases.

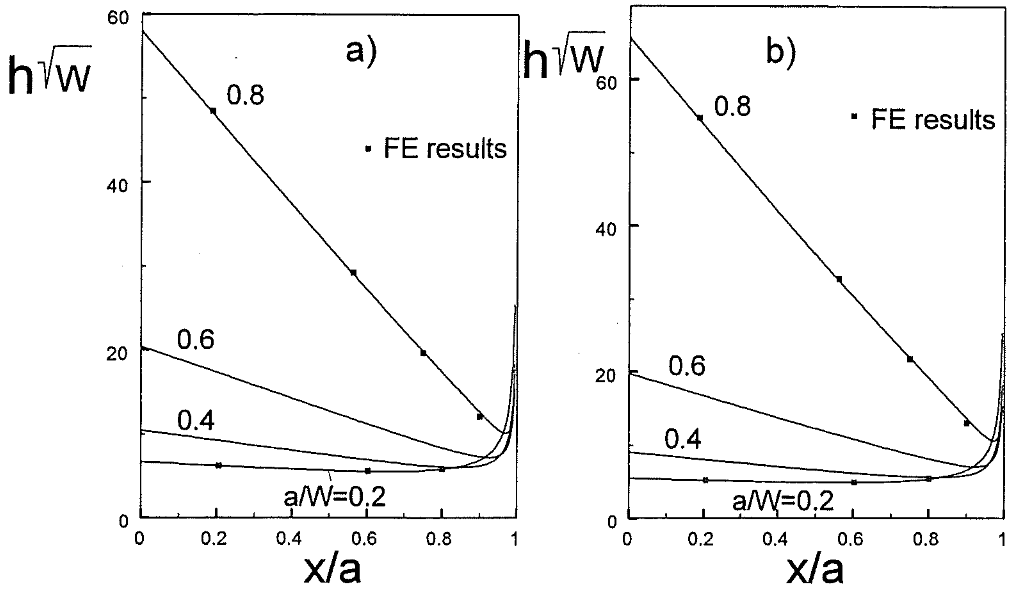

Fig. 13 Comparison of approximate weight functions (curves) with FE results (squares) for transition functions a) eq.(6.13) and b) eq.(6.14).

More complicated transition functions were assumed. As a further example we considered cubic transition functions exhibiting inflection points within the range of $0 < x/W < 1$. Particularly, we considered cases with different points of inflection ($x_0/W = 0.2$, 0,4, 0.6 and 0.8). The transition functions are given by

$$E / E_0 = 1 - A_1 \left[\left(\frac{x_0}{W} \right)^3 + \left(\frac{x}{W} - \frac{x_0}{W} \right)^3 \right] \tag{6.15}$$

with the coefficients A_1=1.88462 for $x_0/W = 0.2$ and 0.8 and $A_1 = 3.5$ for $x_0/W = 0.4$ and 0.6. The four transition functions are shown in Fig. 14. The circles represent the points of inflection.

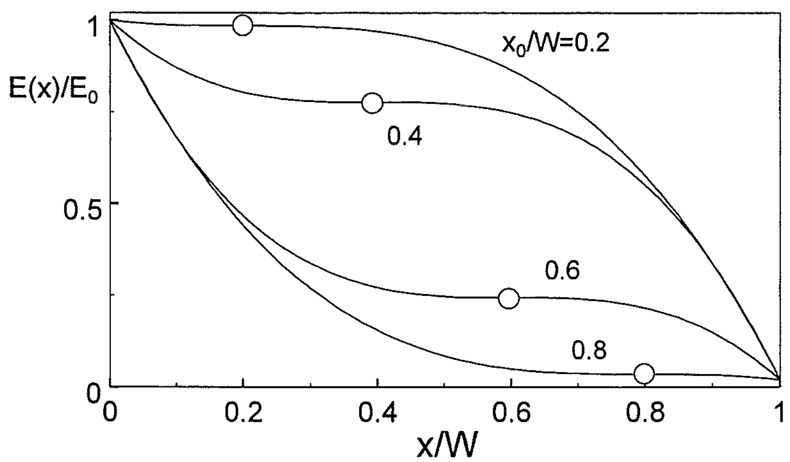

Fig. 14 Transition functions for the Young's modulus according to eqs.(6.15), circles: points of inflection.

Weight functions with 4 terms were computed according to eqs.(6.6) and (6.7) for the transition function (6.15). The results are plotted in Fig. 15. In this illustration the data for special crack lengths, namely $a/W = x_0/W$, were chosen. A comparison of the curves with FE results (squares) shows a good agreement also for these transition functions.

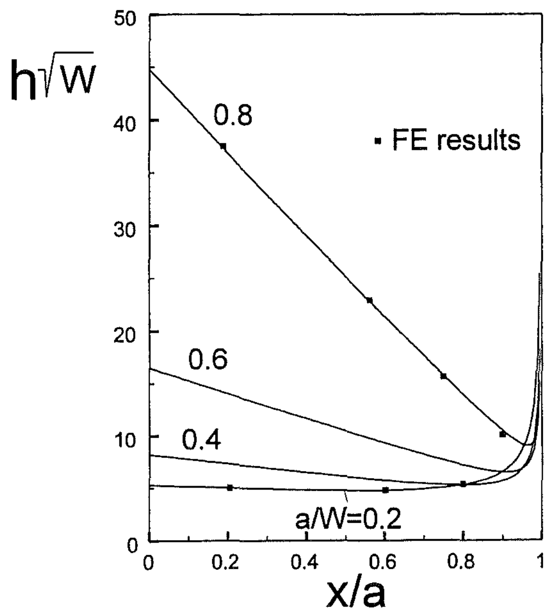

Fig. 15 Weight functions for the transition functions represented by Fig. 14 and crack depths chosen as $a=x_0$. Curves: eq.(6.15), squares: FE results.

7 Conclusions

From the analytical and numerical considerations, it can be concluded that

(1) the Rice equation between displacements and weight function is valid also in the case of graded materials, where the Young's modulus at the crack tip has to be introduced for E,

(2) the approximate procedures for the derivation of weight functions (Petroski Achenbach [19] method and direct adjustment [23] procedure) are valid also in case of graded materials.

In the case of the Petroski Achenbach procedure

- the Young's modulus at the crack tip has to be used for all near-tip considerations.
- As a modification of homogeneous materials in the energy condition (condition of self-consistency), the Young's modulus has to be drawn under the integral.
- The condition of the disappearing second derivative of crack opening displacements ($v''=0$ at $x=y=0$) remains unaffected by the E-gradient.

In the case of the direct adjustment of weight functions to reference stress intensity factor solutions, no change is necessary compared with the procedure for homogeneous materials. Therefore, the application of this method is recommended.

For a wide range of possible transition functions for the change in Young's modulus, approximate weight functions were determined. A comparison of the results with finite element data showed best agreement for all transition functions.

Acknowledgement:

This study was supported by the Deutsche Forschungsgemeinschaft.

8 References

[1] Proceedings of the First International Symposium, FGM, Sendai, Japan 1990, Eds. M. Yamanouchi, M. Koizumi, T. Hirai, I. Shiota.

[2] Ceramic Transactions, Functionally Gradient Materials, 34, Westerville, USA, 1992, Eds. J.B. Holt, M. Koizumi, T. Hirai, Z.A. Munir.

[3] Proceedings of the Third International Symposium, FGM, Lausanne, Switzerland, 1994, Eds. B. Ilschner, N. Cherradi.

[4] Proceedings of the Fourth International Symposium, FGM, Tsukuba, Japan, 1996, Eds. I. Shiota, Y. Miyamoto.

[5] Eischen, J.W., Fracture of nonhomogeneous materials, Int. J. Fract. **34**(1987), 3-22.

[6] Ang, W.T., Clements, D.L., On some crack problems for inhomogeneous elastic materials, Int. J. Solids&Struct. **23**(1987), 1089-1104.

[7] Erdogan, F., Fracture problems in FGMs and application to graded interfaces and coatings, Proc. First Intern. Symp. FGM, Sendai 1990, 307-312.

[8] Ozturk, M., Erdogan, F., The axisymmetric crack problem in a nonhomogeneous medium, J. Appl. Mech. **60**(1993), 406-413.

[9] Erdogan, F., Wu, B.H., Analysis of FGM specimens for fracture toughness testing, in: Ceramic Transactions, Vol. 34: Functionally Gradient Materials (ed. by J.B. Holt et al.), 39-46.

[10] Jin, Z.-H., Noda, N., Minimization of thermal stress intensity factor for a crack in a metal-ceramic mixture, in: Ceramic Transactions, Vol. 34: Functionally Gradient Materials (ed. by J.B. Holt et al.), 47-54.

[11] Jin, Z.-H., Noda, N., Transient thermal stress intensity factors for a crack in a plate of a functionally gradient material, Int. J. Solids&Structures **31**(1994), 203-218.

[12] Bleek, O., Munz, D., Schaller, W., Yang, Y.Y., Effect of a graded interlayer on the stress intensity factor of cracks in a joint under thermal loading, Engng. Fract. Mech. **60**(1998), 615-623.

[13] Fett, T., Munz, D., Stress intensity factors and weight functions, Computational Mechanics Publications, Southampton, 1997.

[14] Fett, T., Munz, D., A weight function for cracks in gradient materials, Int. J. Fract. **84**(1997), L3-L7.

[15] Bückner, H., A novel principle for the computation of stress intensity factors, ZAMM **50**(1970), 529-546.

[16] Rice, J.R., Some remarks on elastic crack-tip stress fields, Int. J. Solids and Structures **8**(1972), 751-758.

[17] Tada, H., Paris, P.C., Irwin, G.R., The stress analysis of cracks handbook, Del Research Corporation, 1986.

[18] Murakami, Y., et al., Stress Intensity Factors Handbook, Vol. 3, Pergamon Press, Oxford, 1986.

[19] Petroski, H.J., Achenbach, J.D., Computation of the weight function from a stress intensity factor, Engng. Fract. Mech. **10**(1978), 257.

[20] Wu, X.R., Carlsson, A.J., Weight functions and stress intensity factor solutions, Pergamon Press, Oxford 1991.

[21] Fett, T., Mattheck, C., Munz, D., Crack opening displacement from the stress intensity factor, Engng. Fract. Mech. **27**(1987), 697-715.

[22] Fett, T., Conditions for the determination of approximative COD fields, Engng. Fract. Mech. **39**(1991), 905-914.

[23] Fett, T., Direct determination of weight functions from reference loading cases and geometrical conditions, Engng. Fract. Mech. **42**(1992), 435-444.

[24] Erdogan, F., Crack problems in nonhomogeneous materials, in: FRACTURE, A Topical Encyclopedia (G. P. Cherepanov) Chapter 5, pp. 72-98, Malabar, Florida, 1998.

[25] Erdogan, F., Fracture mechanics of functionally graded materials, Compos. Engng. **5**(1995), 753-770.

[26] Williams, M.L., On the stress distribution at the base of a stationary crack, J. Appl. Mech. **24** (1957), 109-114.

[27] Irwin, G.R., Analysis of stresses and strains near the end of a crack transversing a plate, J. Appl. Mech. **24**(1957), 361.

[28] Fett, T., Diegele, E., Rizzi, G., Munz, D., Weight functions for edge cracks in thin surface layers, Int. J. Fract. **81**(1996), 205-215.